



## Study of excited B-mesons

The DØ Collaboration

URL: <http://www-d0.fnal.gov>

(Dated: August 1, 2004)

Excited B mesons  $B_1$  and  $B_2^*$  are observed directly for the first time as two separate states in fully reconstructed decays to  $B^{(*)}\pi$ . The mass of  $B_1$  is measured to be  $5724 \pm 4 \pm 7 \text{ MeV}/c^2$  and the mass difference  $\Delta M$  between  $B_2^*$  and  $B_1$  is  $23.6 \pm 7.7 \pm 3.9 \text{ MeV}/c^2$ .

*Preliminary Results for Summer 2004 Conferences*

## I. INTRODUCTION

The spectroscopy of mesons containing  $b$ -quark has not been well studied. Only the  $J^P = 0^-$  ground states  $B^+$ ,  $B_d^0$ ,  $B_s^0$ , and the  $J^P = 1^-$  excited state  $B^*$  are considered as established by the PDG [1]. Almost all observations of the narrow  $L = 1$  states  $B_1$  and  $B_2^*$  were done indirectly in inclusive or semi-inclusive decays [2–5], which prevented their separation and the precise measurement of their properties. The measurement of ALEPH [6], although partially done with exclusive  $B$  decays, was statistically-limited and model-dependent. The masses, widths, and decay branching fractions of these states, on the contrary, are predicted with good precision by various theoretical models [7–10]. These predictions can be verified experimentally, and such comparison can provide important information on the quark interaction inside bound states and help in further development of the non-perturbative QCD. This note presents the study of narrow  $L = 1$  states decaying to  $B^{(*)}\pi$  with exclusively reconstructed  $B$  mesons using the statistics collected in the DØ experiment during 2002-2004 and corresponding to a total integrated luminosity of  $350 \text{ pb}^{-1}$ .

## II. EVENT ANALYSIS

The  $B^+$  and  $B_d^0$  mesons were reconstructed in the following final states:

$$B^+ \rightarrow J/\psi K^+; \quad (1)$$

$$B_d^0 \rightarrow J/\psi K^{*0}; \quad (2)$$

$$B_d^0 \rightarrow J/\psi K_S. \quad (3)$$

The parameters of reconstructed  $B$  mesons in these decays are given in Table I. The details of the criteria used to select these states can be found in [11]. Fig. 1 shows the corresponding mass plots.

The obtained sample of  $B$  mesons was used to select the  $B_J \rightarrow B^{(*)}\pi$  decay. The analysis in each  $B$  decay channel was almost identical with minor variations. For each reconstructed  $B$  meson candidate, an additional track having hits in both the silicon tracker and the central fiber tracker, and transverse momentum exceeding the  $p_T^{min}$  value was selected. Correct charge correlation ( $B^+\pi^-$  or  $B^-\pi^+$ ) was required for channel (1), and no charge correlation was imposed for the other two channels. Since  $B_J$  decays immediately after production, the additional track was required to originate from the primary interaction point by applying the condition on its combined significance  $S_{PV}^2 < C$ , where  $S_{PV}^2 = (d_{ax}/\sigma_{ax})^2 + (d_{st}/\sigma_{st})^2$ . In this expression  $d_{ax}$ ,  $d_{st}$  are the axial and stereo impact parameters with respect to the primary vertex, and  $\sigma_{ax}$ ,  $\sigma_{st}$  are their errors. Table II gives the specific values of cuts used. Tighter selection in decay channel (2) was motivated by higher background under the  $B$  meson, see Fig.1.

For each track in an event satisfying the above criteria, the mass difference  $\Delta M = M(B\pi) - M(B)$  was computed. The resulting distribution of the  $\Delta M$  is shown in Fig. 2. The mass difference between charged and neutral  $B_J$  mesons is expected to be negligible compared to the experimental resolution in  $\Delta M$ . For the  $0^-$  neutral and charged  $B$  mesons this mass difference is only  $0.33 \pm 0.28 \text{ MeV}/c^2$  [1]. Therefore, the contributions from all three channels (1-3) were combined together in Fig. 2.

Fig. 2 reveals a complicated structure for  $\Delta M$  around 430 MeV, which can be interpreted as the decay  $B_J \rightarrow B^{(*)}\pi$ . The dominant decay mode of  $B_1$  meson should be  $B_1 \rightarrow B^*\pi$ , while the decay  $B_1 \rightarrow B\pi$  is forbidden by angular momentum and parity conservation.  $B_2^*$  can decay both to  $B^*\pi$  and  $B\pi$  with the relative rate 1:1 predicted by the theory.  $B^*$  decays to  $B\gamma$  with 100 % probability. Since the mass difference of  $B^*$  and  $B$  is only  $45.78 \pm 0.35 \text{ MeV}/c^2$  [1], the  $\Delta M$  for  $B_J \rightarrow B^*\pi$  decays is:

$$\Delta M = M(B\pi) - M(B) \simeq M(B\pi\gamma) - M(B\gamma) = M(B_J) - M(B^*). \quad (4)$$

This expression shows that the signal from  $B_J \rightarrow B^*\pi$  in the mass difference  $M(B\pi) - M(B)$  should be shifted relative to the signal from  $B_J \rightarrow B\pi$  by  $\sim 46 \text{ MeV}/c^2$ . The simulation shows that the width of  $\Delta M$  distribution both for  $B_J \rightarrow B^*\pi$  and  $B_J \rightarrow B\pi$  is almost the same. Therefore, decays of  $B_J$  should produce three peaks in

TABLE I: Parameters of selected exclusive  $B$  meson decays. All errors given are statistical only.

decay	reconstructed mass (MeV/ $c^2$ )	mass resolution (MeV/ $c^2$ )	number of events
$B^+ \rightarrow J/\psi K^+$	$5271 \pm 0.7$	$41.6 \pm 0.8$	$7217 \pm 127$
$B_d^0 \rightarrow J/\psi K^{*0}$	$5271 \pm 1.3$	$37.6 \pm 1.3$	$2826 \pm 93$
$B_d^0 \rightarrow J/\psi K_S$	$5281 \pm 1.8$	$29.0 \pm 1.8$	$624 \pm 41$

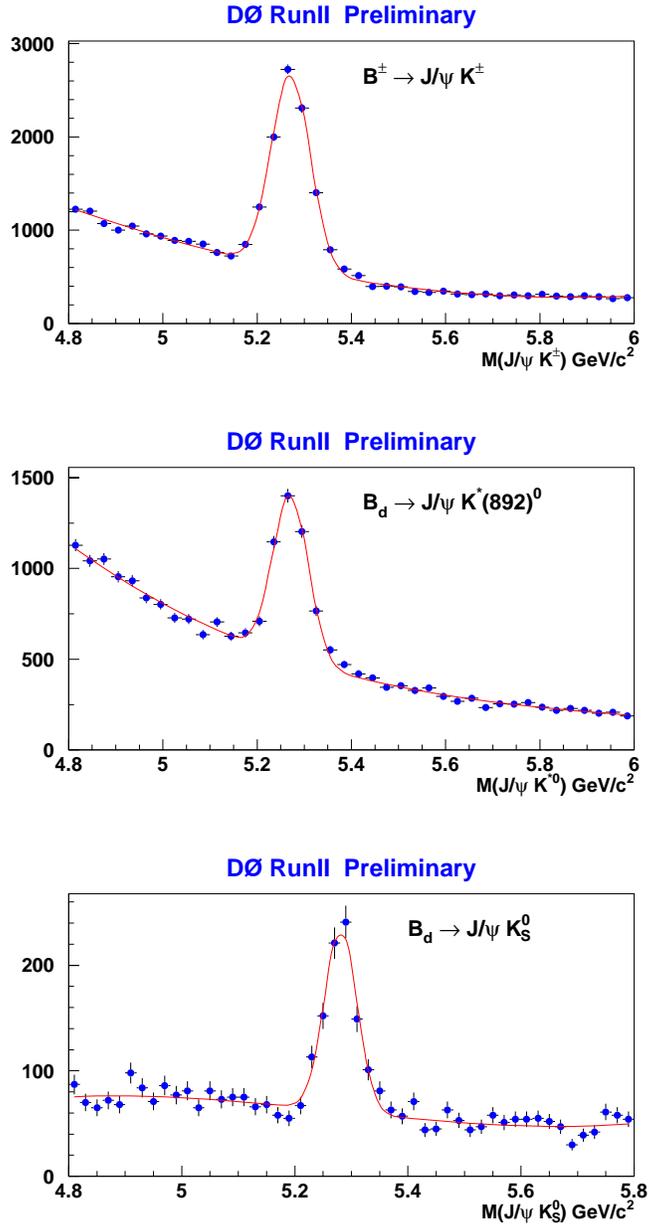


FIG. 1: Mass distributions of  $J/\psi K^+$ ,  $J/\psi K^{*0}$  and  $J/\psi K_S$  events. The line shows the fit by the sum of Gaussian and polynomial background.

the  $\Delta M$  distribution with the central positions  $\Delta_1 = M(B_1) - M(B^*)$ , corresponding to the decay  $B_1 \rightarrow B^* \pi$ ,  $\Delta_2 = M(B_2^*) - M(B^*)$ , corresponding to  $B_2^* \rightarrow B^* \pi$ , and  $\Delta_3 = M(B_2^*) - M(B)$ , corresponding to  $B_2^* \rightarrow B \pi$ . Since the mass difference between  $B_2^*$  and  $B_1$  is expected to be small comparing to the detector resolution, the first two peaks are observed as the single structure.

In addition to the narrow  $L = 1$  states, there should be two wide  $B_J$  states decaying to  $B^{(*)} \pi$  through the  $S$ -wave. However, all theoretical models [7–10] predict their width to be too large, up to  $1 \text{ GeV}/c^2$ , so that they can't be distinguished from the non-resonant background with the current statistics.

Following this expected pattern, the experimental distribution was fitted by the following function:

$$\begin{aligned}
 F(\Delta M) &= F_{sig}(\Delta M) + F_{back}(\Delta M); \\
 F_{sig}(\Delta M) &= N \cdot (f_1 \cdot G(\Delta M, \Delta_1, \Gamma_1) + (1 - f_1) \cdot (f_2 \cdot G(\Delta M, \Delta_2, \Gamma_2) + (1 - f_2) \cdot G(\Delta M, \Delta_3, \Gamma_2))). \quad (5)
 \end{aligned}$$

In these equations,  $\Gamma_1$  and  $\Gamma_2$  are the widths of  $B_1$  and  $B_2^*$ ,  $f_1$  is the fraction of  $B_1$  contained in the  $B_J$  signal and  $f_2$  is the branching decay rate of  $B_2^* \rightarrow B^* \pi$ . The parameter  $N$  gives the total number of observed  $B_J \rightarrow B^{(*)} \pi$  decays.

TABLE II: Selection criteria for  $B_J \rightarrow B^{(*)}\pi$  decay

selection	$B^+ \rightarrow J/\psi K^+$	$B_d^0 \rightarrow J/\psi K^{*0}$	$B_d^0 \rightarrow J/\psi K_S$
$B\pi$ charge correlation	yes	no	no
$B$ mass range (GeV/ $c^2$ )	5.19–5.34	5.22–5.34	5.22–5.34
$p_T^{min}$ (GeV/ $c$ )	0.7	0.9	0.7
$C$	6	6	6

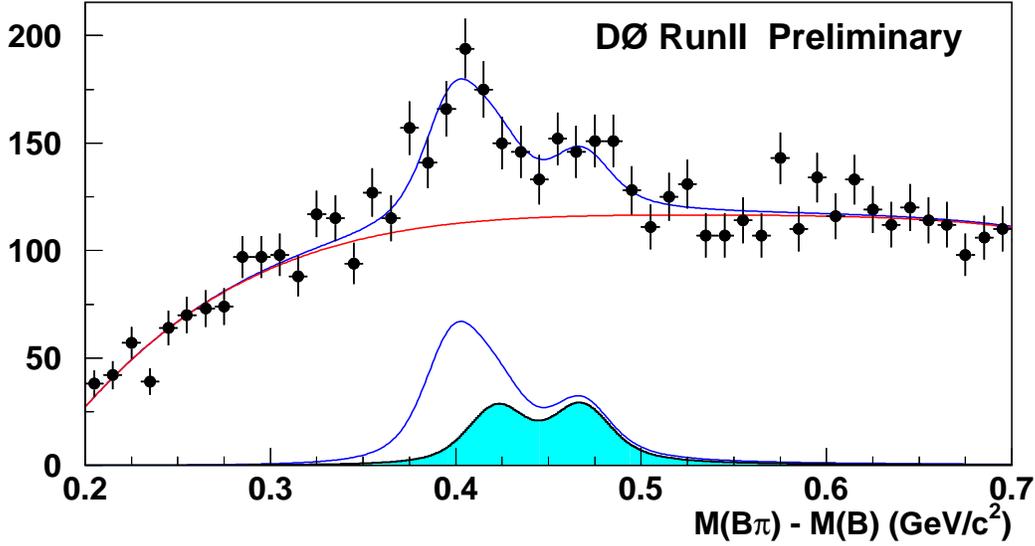


FIG. 2: Mass difference  $\Delta M = M(B\pi) - M(B)$  for exclusive  $B$  decays. The upper blue curve shows the fit by function (5). The red line is the background contribution. The lower blue line shows the signal with the background subtracted, and the filled histogram shows the contribution of  $B_2^* \rightarrow B^*\pi$  and  $B_2 \rightarrow B\pi$  decays.

The background  $F_{back}(\Delta M)$  was parameterized by a polynomial. The function  $G(x, x_0, \Gamma)$  is the convolution of a relativistic Breit-Wigner function with the experimental resolution in  $\Delta M$ , parameterized as a Gaussian:

$$G(x, x_0, \Gamma_0) = \frac{1}{\sqrt{2\pi}\sigma} \cdot \frac{1}{N_0} \int \exp\left(\frac{-(x-x')^2}{2\sigma^2}\right) \cdot \frac{x_0\Gamma(x)}{(x'^2 - x_0^2)^2 + x_0^2\Gamma^2(x)} dx'; \quad (6)$$

$$N_0 = \int \frac{x_0\Gamma(x)}{(x^2 - x_0^2)^2 + x_0^2\Gamma^2(x)} dx; \quad (7)$$

$$\Gamma(x) = \Gamma_0 \frac{x_0}{x} \left(\frac{k}{k_0}\right)^{2L+1} F^{(L)}(k, k_0) \quad (L=2); \quad (8)$$

$$F^{(2)}(k, k_0) = \frac{9 + 3(k_0r)^2 + (k_0r)^4}{9 + 3(kr)^2 + (kr)^4}. \quad (9)$$

The variables  $k, k_0$  in (8-9) are the magnitude of the pion three-momentum in the  $B_J$  rest frame when  $B_J$  has a four-momentum-square equal to  $x^2$  and  $x_0^2$  respectively,  $F^{(2)}(k, k_0)$  is the Blatt-Weiskopf form factor for  $L=2$  decays [12], and  $r = 5 \text{ (GeV}/c)^{-1}$  is a hadron scale. The  $L=2$  corresponds to the  $D$ -wave decays of  $B_J$ .

All theoretical models predict very close widths  $\Gamma_1$  and  $\Gamma_2$  of  $B_1$  and  $B_2^*$ . Therefore, they were set to be equal in the fit:  $\Gamma_1 = \Gamma_2 = \Gamma$ . The  $f_2$  was fixed at 0.5 following the theoretical expectations. The experimental resolution, obtained from simulation, was  $\sigma = 10.3 \pm 0.6 \text{ MeV}/c^2$ , where the error represents the uncertainty from the simulation

TABLE III: The correlation coefficients between fitted parameters

parameter	$N$	$f_1$	$M(B_1)$	$M(B_2^*) - M(B_1)$	$\Gamma$
$N$	1.000	-0.054	-0.269	0.282	0.704
$f_1$	-0.054	1.000	0.553	0.196	0.224
$M(B_1)$	-0.269	0.553	1.000	-0.250	-0.055
$M(B_2^*) - M(B_1)$	0.282	0.196	-0.250	1.000	0.008
$\Gamma$	0.704	0.224	-0.055	0.008	1.000

TABLE IV: Systematic uncertainties of  $B_J$  parameters

source	$dM(B_1)$ (MeV/c <sup>2</sup> )	$d(M(B_2^*) - M(B_1))$ (MeV/c <sup>2</sup> )	$d\Gamma_{1,2}$ (MeV/c <sup>2</sup> )	$df_1$
background parameterization	2	2.2	4.5	0.03
$f_2 = [0, 0.7]$	6	3.1	6.2	0.21
$\Gamma_2$ free in the fit	0	0.5	1.4	0.02
$\sigma(\Delta M) \pm 28\%$	2	0.6	7.1	0.03
momentum scale	1	0.1	0	0
total	6.7	3.9	9.3	0.21

statistics only. With these assumptions, the following parameters for  $B_1$  and  $B_2^*$  were obtained:

$$N = 536 \pm 114 \text{ events}; \quad (10)$$

$$M(B_1) = 5724 \pm 4 \text{ MeV}/c^2; \quad (11)$$

$$M(B_2^*) - M(B_1) = 23.6 \pm 7.7 \text{ MeV}/c^2; \quad (12)$$

$$\Gamma = \Gamma_1 = \Gamma_2 = 23 \pm 12 \text{ MeV}/c^2; \quad (13)$$

$$f_1 = 0.51 \pm 0.11; \quad (14)$$

$$\chi^2/NDF = 54.3/50. \quad (15)$$

The errors given are statistical only. Without the  $B_J$  signal contribution, the  $\chi^2$  of the fit is increased by 64, which corresponds to the  $\sim 7\sigma$  statistical significance of observing this structure. Fitting the distribution with only one peak increases the  $\chi^2$  by 16. Table III gives the correlation coefficients between the fitted parameters.

### III. SYSTEMATIC ERRORS AND CONSISTENCY CHECKS

The influence of different sources of systematic uncertainty is given in Table IV and was estimated as follows. Different background parameterizations were tried. The fitting range of the  $\Delta M$  distribution was varied. The parameters describing the background were allowed to vary in the fit, and their error was already included in (10-14). The decay rate  $B_2^* \rightarrow B^* \pi$  was varied between 0 and 0.7. To check the effect of the assumption  $\Gamma_1 = \Gamma_2$ , the widths  $\Gamma_1$  and  $\Gamma_2$  were allowed to vary independently in the fit, and the change in parameters was taken as the systematic error from this source. The detector mass resolution was varied by 28%, which corresponds to the difference between the data and simulation in the measured width of the mass difference  $M(D^{*+}) - M(D^0)$ . In  $D\bar{O}$  the measured mass of  $B$  hadrons is shifted relative to the world average due to an uncertainty in the  $D\bar{O}$  momentum scale, see Table I. The mass differences  $M(B_1) - M(B^*)$  and  $M(B_2^*) - M(B_1)$  were corrected by the ratio of the  $D\bar{O}$  measured mass to the accepted world-average mass of  $B$ -mesons, and a 100% uncertainty was assigned to this mass scale correction. In addition, the fit was repeated without the Blatt-Weiskopf form-factor (9) and no visible change in the results was observed.

Several consistency checks of the observed signal were performed. Figures 3,4 show the  $\Delta M$  distribution separately for channel (1) and for channels (2,3). It can be seen that the  $B_J$  signal is present in both  $B^+ \pi$  and  $B_d \pi^+$  channels. Events with positive and negative pions were analyzed separately. The data set was divided into two parts according to the collection date. In all cases the signal was present in both parts of the sample. The complementary sample of events containing a pion not compatible with the primary vertex was selected by requiring  $S_{PV}^2 > 16$ . No significant signal of  $B_J$  was observed, as can be seen in Fig. 5. The fit with parameters fixed at (10-14) gave  $32 \pm 36$  events, consistent with zero.

## DØ RunII Preliminary

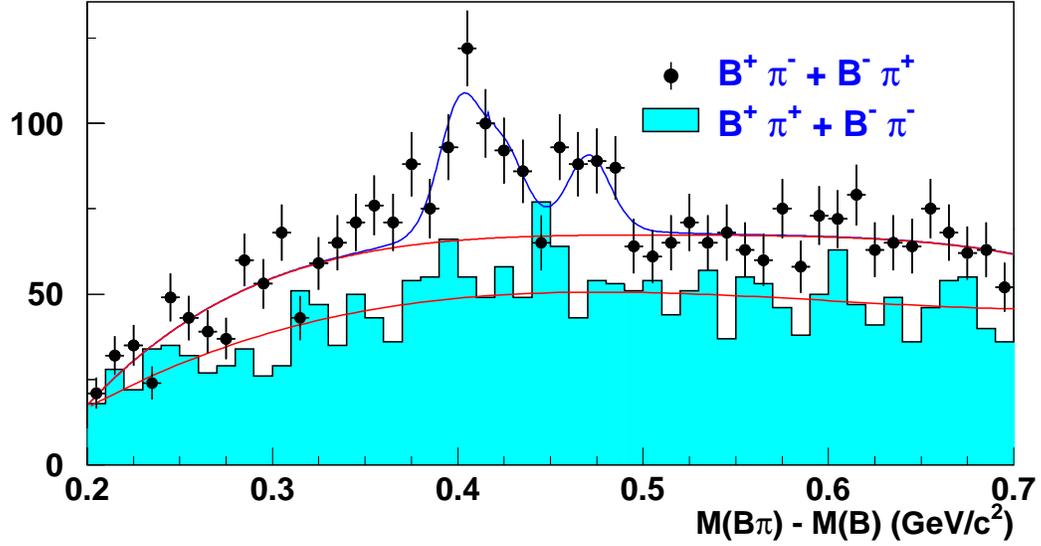


FIG. 3: Mass difference  $\Delta M = M(B\pi) - M(B)$  for  $B^\pm \rightarrow J/\psi K^\pm$  decay. The blue line shows the fit to function (5), and the upper red line is the background contribution. The filled histogram shows the  $\Delta M$  distribution for events with the wrong charge correlation between  $B$  and  $\pi$ . The lower red line shows the fit to the background polynomial for the wrong-sign events.

## DØ RunII Preliminary

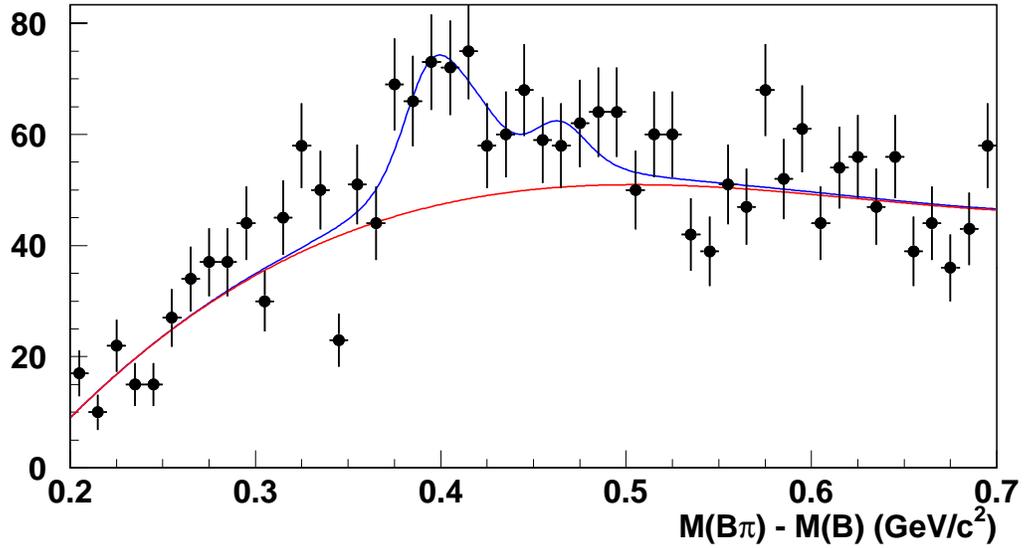


FIG. 4: Mass difference  $\Delta M = M(B\pi) - M(B)$  for  $B_d \rightarrow J/\psi K^{*0}$  and  $B_d \rightarrow J/\psi K_S$  decays. The blue line shows the fit to function (5) and the contribution of the background is shown by the red line.

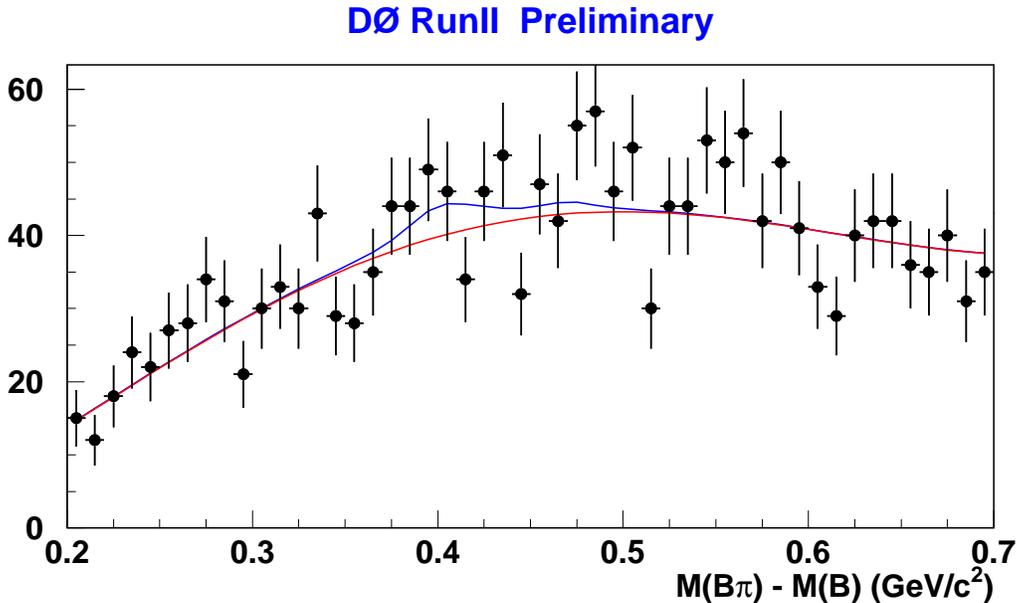


FIG. 5: Mass difference  $\Delta M = M(B\pi) - M(B)$  for events with the pion not compatible with the primary vertex ( $S_{PV}^2 > 16$ ). The line shows the fit by the function (5) with and without the  $B_J$  signal.

#### IV. CONCLUSIONS

In conclusion, the  $B_1$  and  $B_2^*$  are observed for the first time as two separate objects. Their masses and the average width were measured to be:

$$M(B_1) = 5724 \pm 4 \text{ (stat)} \pm 7 \text{ (syst)} \text{ MeV}/c^2; \quad (16)$$

$$M(B_2^*) - M(B_1) = 23.6 \pm 7.7 \text{ (stat)} \pm 3.9 \text{ (syst)} \text{ MeV}/c^2; \quad (17)$$

$$\Gamma_1 = \Gamma_2 = 23 \pm 12 \text{ (stat)} \pm 9 \text{ (syst)} \text{ MeV}/c^2. \quad (18)$$

Further increases in statistics will allow precision measurements of their production and decay properties.

#### Acknowledgments

We thank the staffs at Fermilab and collaborating institutions, and acknowledge support from the Department of Energy and National Science Foundation (USA), Commissariat à l'Énergie Atomique and CNRS/Institut National de Physique Nucléaire et de Physique des Particules (France), Ministry of Education and Science, Agency for Atomic Energy and RF President Grants Program (Russia), CAPES, CNPq, FAPERJ, FAPESP and FUNDUNESP (Brazil), Departments of Atomic Energy and Science and Technology (India), Colciencias (Colombia), CONACyT (Mexico), KRF (Korea), CONICET and UBACyT (Argentina), The Foundation for Fundamental Research on Matter (The Netherlands), PPARC (United Kingdom), Ministry of Education (Czech Republic), Natural Sciences and Engineering Research Council and WestGrid Project (Canada), BMBF (Germany), A.P. Sloan Foundation, Civilian Research and Development Foundation, Research Corporation, Texas Advanced Research Program, and the Alexander von Humboldt Foundation.

- 
- [1] S.Eidelman *et al.* (Particle Data Group), Phys. Lett. **B592**, 1 (2004).  
 [2] OPAL Collab., Z. Phys. **C66**, 19 (1995).  
 [3] DELPHI Collab., Phys. Lett. **B345**, 598 (1995).  
 [4] ALEPH Collab., Z. phys. **C69**, 393 (1996).

- [5] CDF Collab., Phys. Rev. **D64**, 072002 (2001).
- [6] ALEPH Collab., Phys. Lett. **B425**, 215 (1998).
- [7] E.J.Eichten, C.T.Hill, C.Quigg, Phys. Rev. Lett. **71**, 4116 (1993) and an update FERMILAB-CONF-94/118-T.
- [8] N.Isgur, Phys. Rev. **D57**, 4041 (1998).
- [9] D.Ebert, V.O.Galkin, R.N.Faustov, Phys. Rev. **D57**, 5663 (1998), Erratum Phys. Rev. **D59** 019902 (1999).
- [10] A.H.Orsland, H.Hogaasen, Eur.Phys.J. **C9** 503 (1999).
- [11] DØ Note 4481 (2004).
- [12] J.Blatt and V.Weisskopf, Theoretical Nuclear Physics, p.361, New York: John Wiley & Sons (1952).